

Heavy-Mass Fermi Liquid near a Ferromagnetic Instability in Layered Ruthenates

S. Nakatsuji,^{1,2} D. Hall,¹ L. Balicas,¹ Z. Fisk,¹ K. Sugahara,² M. Yoshioka,² and Y. Maeno^{2,3,4}

¹National High Magnetic Field Laboratory (NHMFL), Tallahassee, Florida 32310

²Department of Physics, Kyoto University, Kyoto 606-8502, Japan

³International Innovation Center, Kyoto University, Kyoto 606-8501, Japan

⁴CREST, Japan Science and Technology Corporation, Kawaguchi, Saitama 332-0012, Japan

(Received 20 September 2002; published 2 April 2003)

Low temperature magnetic, thermal, and transport measurements in $\text{Ca}_{2-x}\text{Sr}_x\text{RuO}_4$ clarify the appearance of a cluster glass phase, after the evolution of a nearly ferromagnetic heavy-mass Fermi liquid from the spin-triplet superconductor Sr_2RuO_4 . As the Mott transition is approached across a 2nd-order structural transition, both the magnetization and specific heat decrease considerably while the transport scattering rate diverges. A metamagnetic transition to a highly spin polarized state, with a local moment $S = 1/2$, is observed. We argue that an orbital rearrangement with Ca substitution changes itinerant ferromagnetism to antiferromagnetism of localized moments.

DOI: 10.1103/PhysRevLett.90.137202

PACS numbers: 75.40.-s, 71.30.+h, 74.70.Pq

A diversity of orbital related phenomena has attracted considerable interest in transition metal oxides (TMOs) [1]. Among the TMOs, the single layered ruthenate Sr_2RuO_4 is a rare example of a well-defined Fermi liquid (FL) displaying spin-triplet superconductivity. Extensive studies, initiated by the discovery of superconductivity [2], revealed its complex “orbital dependent” physics [3]. The normal state is a quasi-2D FL whose Fermi surfaces are composed of three warped cylinders, originating from the $4dt_{2g}$ orbitals in the RuO_2 planes [4,5]. The α and β Fermi surfaces arise from 1D chains of $d_{yz,zx}$ orbitals while the γ sheet originates from a 2D network of planar d_{xy} orbitals. This difference in dimensionality, as well as in their parity under reflection with respect to RuO_2 planes, defines its unique orbital dependent properties.

Band structure calculations [6,7] predict two competing magnetic instabilities in the normal state: an incommensurate antiferromagnetic (AF) order due to the nesting within the $d_{yz,zx}$ (α , β) bands and a ferromagnetic (FM) instability due to the van Hove singularity in the d_{xy} (γ) band. The incommensurate spin fluctuations have been confirmed by neutron scattering measurements [8], leading to theoretical studies on their relevant role in the superconducting mechanism [9]. In contrast, no FM fluctuations have been detected in neutron studies [8], while NMR results show a weak exchange enhancement [10,11]. In the superconducting state, however, the prominent role of the γ band has been pointed out by experimental and theoretical studies [3,12]. It has been suggested that the main gap opens in the active γ band, inducing the superconductivity in the α and β bands by proximity effect. A FM fluctuation mediated superconductivity in the γ band has been proposed [6,7,13].

Although no clear indication of FM fluctuations is yet found in Sr_2RuO_4 , the FM coupling in the γ band has been recently suggested based on studies of $\text{Ca}_{2-x}\text{Sr}_x\text{RuO}_4$ [14–16]. In this system, the substitution

with isovalent Ca increases the effective electron correlations by introducing structural distortions and, thus, may develop orbital dependent magnetism.

Starting from undistorted Sr_2RuO_4 , Ca substitution initially stabilizes the rotation of RuO_6 octahedra and induces an enhancement of the low- T susceptibility χ . Surprisingly, $\chi(T)$ shows divergent Curie behavior near a structural instability at a critical value $x_c \approx 0.5$ where recent polarized neutron diffraction measurements under field [16] revealed an anomalously large magnetization density at both Ru and O in-plane sites. The strongly anisotropic density at the Ru sites, similar to the distribution of the d_{xy} orbital, suggests a FM instability due to the dominant influence of the van Hove singularity of the γ band, as predicted by band structure calculations [7]. Nevertheless, $\chi(T)$ is strongly suppressed by the appearance of a metallic region with AF coupling (which we refer to as the magnetic metallic region) as the Mott transition at $x \approx 0.2$ is approached through the structural transition at x_c . Finally, the complete substitution of Sr by Ca changes the superconductor into the Mott insulator Ca_2RuO_4 [17,18]. The strong Jahn-Teller distortion and its resultant orbital polarization indicate an orbital ordering in the AF insulating state [15,19–21].

The significant structural dependence of the magnetism in this system, particularly the FM coupling in the γ band, the probable active band for superconductivity, suggests a strong “orbital dependence” of its physical properties. This is also featured by a recent discovery of the pressure-induced FM metallic phase in Ca_2RuO_4 [22]. In this Letter, we present the magnetic, thermal, and transport properties of $\text{Ca}_{2-x}\text{Sr}_x\text{RuO}_4$ under zero and finite magnetic fields at low temperatures. Our purpose is twofold: (i) to examine the presence of the FM instability around $x = 0.5$ predicted by theory and to clarify how it develops from the spin-triplet superconductor, and (ii) to study the evolution of the orbital dependent

magnetism in the metallic state, particularly in the vicinity of the orbital ordered Mott insulating phase.

Single crystals were prepared using a floating zone method [14]. X-ray powder diffraction patterns show single phase samples. The notations for the unit cell are assigned using those of $I4/mmm$ symmetry. Magnetization M above 1.8 K was measured with a commercial SQUID magnetometer, while for measurements down to 0.3 K, a magnetometer was constructed using a dc SQUID probe in conjunction with a ^3He refrigerator. To study the field dependence of M , a vibrating sample magnetometer was used, while field dependent four terminal resistivity measurements were performed in a dilution refrigerator, both at the NHMFL. Specific heat C_P was measured by a thermal relaxation method down to 0.35 K.

Figure 1(a) shows the T dependence of the electronic part of the specific heat C_e divided by T for

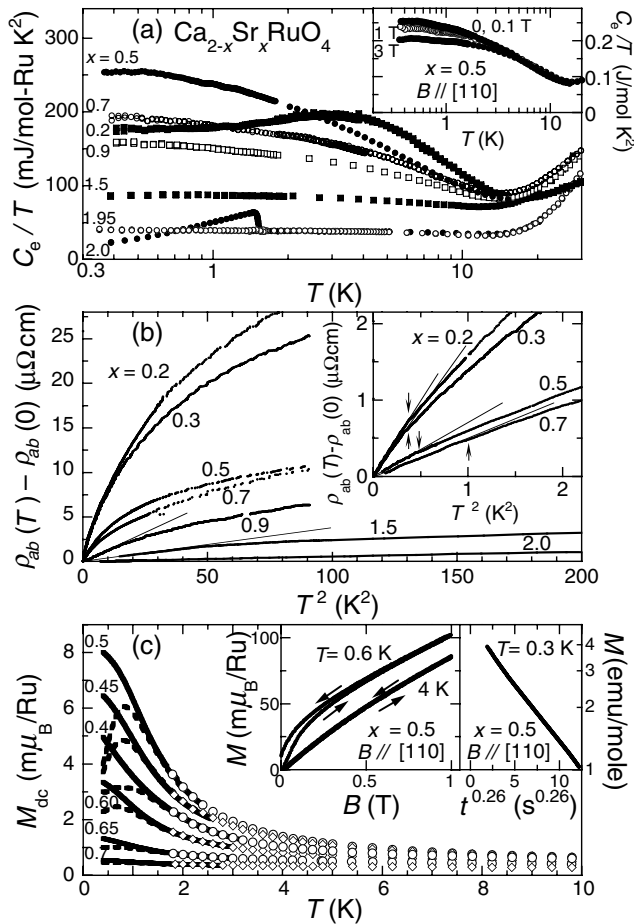


FIG. 1. Low temperature properties of single crystals of $\text{Ca}_{2-x}\text{Sr}_x\text{RuO}_4$. (a) C_e/T vs $\ln T$. Inset: C_e/T for $x = 0.5$ under fields. (b) $\rho_{ab}(T) - \rho_{ab}(0)$ vs T^2 . The low- T parts are enlarged in the inset. The arrows indicate T_{FL} . (c) In-plane M vs T under $B = 10$ mT. Solid and broken lines give FC and ZFC results, respectively. Results measured by the homebuilt SQUID (line) are smoothly connected to the high- T results (open symbol) by a commercial SQUID magnetometer. Insets: M vs B (left) and relaxation curve of M (right) for $x = 0.5$.

$\text{Ca}_{2-x}\text{Sr}_x\text{RuO}_4$. To obtain C_e , we assume that C_P of the insulator Ca_2RuO_4 reasonably represents the lattice contribution for the following two reasons: first, the low temperature C_P/T of the isostructural Ca_2RuO_4 has no electronic part and is well described by βT^2 with almost the same Debye temperature $\Theta_D = 411$ K as Sr_2RuO_4 (410 K); second, any magnetic contribution should be negligible at T well below 110 K, the Néel point. Thus, by subtracting C_P/T of Ca_2RuO_4 , we estimate C_e/T for each x as in Fig. 1(a). Sr_2RuO_4 exhibits a jump in C_e/T because of the superconducting transition at $T_c \approx 1.5$ K. Reflecting its FL state [4,5], C_e/T is constant down to T_c for $x = 2$ and also down to 0.35 K for $x = 1.95$ where 2.5% Ca substitution suppresses T_c . Starting from this well-defined FL behavior, the T dependence of C_e/T systematically enhances with decreasing x . While C_e/T for $x = 1.5$ still displays a T independent FL behavior below ~ 5 K, C_e/T for $x = 0.9, 0.7$, and 0.5 exhibits a significant increase on cooling, showing a FL-like saturation only below $T \approx 0.5$ K. In the magnetic metallic region, a peak is observed, as seen in the trace for $x = 0.2$.

Figure 1(b) shows the inelastic component of the in-plane resistivity $\rho_{ab}(T) - \rho_{ab}(0)$ vs T^2 for the entire metallic region, while the inset shows the low- T part for $x \approx 0.5$ in an enlarged scale. Consistent with the C_e/T results, we found a systematic decrease of the temperature T_{FL} below which a T^2 dependence appears. Starting from ~ 20 K for Sr_2RuO_4 , T_{FL} rapidly decreases down to ~ 0.5 K for $x < 0.5$ [see Fig. 2(a)], where a $T^{1.4}$ dependence appears at higher T on heating [14]. In strongly correlated electron systems, especially in the heavy fermions, the T^2 coefficient A and the electronic specific heat coefficient γ_e obey an empirical relation $A \propto \gamma_e^2$ with a universal ratio $a_0 \equiv A/\gamma_e^2 \approx 1.0 \times 10^{-5} \mu\Omega\text{cm}/(\text{mJ/mol K})^2$ [4,23]. From this relation, we calculated the expected γ_e value $\sqrt{A/a_0}$ in order to compare with $\gamma_e \equiv C_e/T$ (0.4 K) [see Fig. 2(b)]. In the region $2 \geq x \geq 0.5$, both γ_e and $\sqrt{A/a_0}$ agree quite well, suggesting that the same renormalized quasiparticles govern both the enhancement of γ_e and the electrical transport. In fact, the critical enhancement of γ_e , reaching an enormous maximum of $255 \text{ mJ/mol-Ru K}^2$ at $x = 0.5$, indicates the formation of heavy-mass quasiparticles. To our knowledge, this value is the largest ever reported for TMOs, surpassing the value $\gamma_e \approx 210 \text{ mJ/mol-V K}^2$ for LiV_2O_4 [24]. In contrast, for $0.5 > x \geq 0.2$, $\sqrt{A/a_0}$ increases while the actual γ_e decreases, signaling a significant change in the electronic structure across the structural transition. Despite this decrease, the magnitude of γ_e in this region is still 1 order larger than those (10–15 mJ/mol K^2) expected from band calculations [7], indicating a strong correlation effect. A detailed study focused on $x = 0.3$ also revealed heavy-electron behavior [25].

Given that the measured $\chi(T)$ is dominated by renormalized quasiparticles, we calculated the Wilson ratio $R_W = (\pi^2 k_B^2 / 3 \mu_B^2) / (\chi / \gamma_e)$ [see Fig. 2(b)]. Here, χ and γ_e were estimated from their values at 1.8 K where the

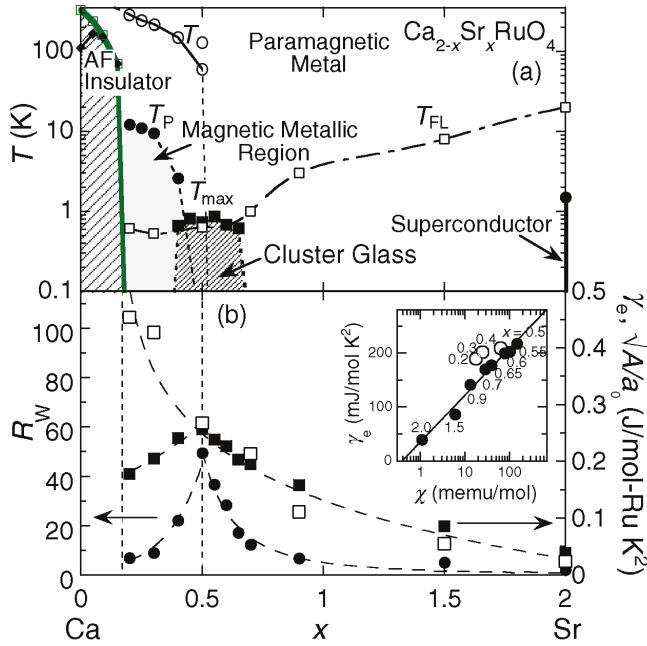


FIG. 2 (color online). (a) Newly found cluster glass phase added to the phase diagram of $\text{Ca}_{2-x}\text{Sr}_x\text{RuO}_4$ from Refs. [14,15]. T_0 and T_P are the structural transition temperature and the peak temperature of $\chi(T)$, respectively. For T_{FL} and T_{max} , see text. (b) The Sr concentration dependence of $\gamma_e \equiv C_e/T$ (0.4 K) (solid square), $\sqrt{A/a_0}$ (open square), and the Wilson ratio R_w (solid circle). The broken lines are guides to the eye. Inset: γ_e vs $\ln\chi$ at 1.8 K. The solid line is a linear fit.

entire metallic region is paramagnetic. While R_w for Sr_2RuO_4 is 2 corresponding to its strongly correlated FL state [4], R_w diverges for $x = 0.5$, reaching a value ≥ 40 which surpasses those known for nearly FM metals, such as Pd (5.8) and TiBe_2 (12) [26]. Furthermore, the inset in Fig. 2(b) indicates that the relation $\gamma_e \propto \ln\chi$ holds in the metallic region for $x \geq 0.5$ including Sr_2RuO_4 . This critical relation is expected for a FL near to Stoner-type FM [27]. Thus, this increase of R_w in the tetragonal phase ($x \geq x_c$) indicates the progressive evolution of a Fermi liquid toward FM. This enhancement of FM correlation was also found by NMR measurements [28].

To characterize the nearly FM state around $x = 0.5$, we have measured the in-plane dc magnetization down to $T = 0.3$ K. Figure 1(c) gives the results of $M(T)$ taken upon heating in the field-cooling (FC) and zero-field-cooling (ZFC) sequences under $B = 10$ mT. At $x = 0.5$, $M(T)$ exhibits FM-like hysteresis below ~ 1.5 K, showing a large enhancement up to $8 \text{ m}\mu_B$. Moreover, the B dependence of M also shows hysteresis at 0.6 K, indicating the appearance of a weak FM component of around $10 \text{ m}\mu_B$ [Fig. 1(c), left inset]. However, this low- T phase possesses a glassy nature as demonstrated by the time dependence of the magnetization. A stretched exponential decay of $M \propto \exp[-(t/\tau)^{0.26}]$ with $\tau = 2800$ s is observed by cooling down to 0.3 K under $B = 10$ mT and removing this field after waiting for a period of 3000 s [Fig. 1(c), right inset]. This indicates that the system is a

cluster glass; the formation of clusters with FM short-range order enhances $M(T)$ until the clusters freeze below the peak temperature T_{max} of the ZFC curve. Both dc- M and T_{max} decrease continuously as x moves away from 0.5 and T_{max} is lowered below 0.3 K at $x \approx 0.3, 0.7$ [see Fig. 1(c)]. This systematic behavior demonstrates that the FM cluster formation is a bulk effect. T_{max} vs x is summarized in Fig. 2(a), showing the cluster glass region in the phase diagram. No anomaly in $\rho(T)$, and only a very weak kink in C_e/T [e.g., at 0.5 K for $x = 0.5$ in Fig. 1(a)] were detected as a spin freezing effect, probably because of the weak FM moments. In addition, the inset in Fig. 1(a) shows that C_e/T is little affected for $B \leq 1$ T and at 3 T reduced only by $\sim 20\%$. This weak dependence on the field of the energy scale of spin freezing ($k_B T_{max}/2\mu_B \sim 1$ T) confirms that the enhancement of C_e/T results from the quasiparticle mass renormalization, not from spin freezing.

Once Ca substitution stabilizes the orthorhombic phase for $x < x_c$, AF coupling appears, leading to the creation of a magnetic metallic region and rapidly suppressing the FM cluster glass. This indicates that the magnetic coupling changes from FM to AF at the 2nd-order structural transition [14,15]. Moreover, this competition between both couplings should generate frustration among the clusters, preventing long-range order.

In the tetragonal phase, the RuO_6 octahedra remain rigid despite their rotation, keeping essentially the same crystal field and hence the triple degeneracy of the t_{2g} orbitals as in Sr_2RuO_4 [6,7,15,20]. However, the tilting of the octahedra in the orthorhombic phase involves a Jahn-Teller distortion. It elongates the RuO_2 planes along the [110] direction and lifts the degeneracy of d_{yz} and d_{zx} orbitals, most probably stabilizing a $d_{yz} - d_{zx}$ state [14]. This Jahn-Teller distortion is sizable ($> 1\%$ at $x = 0.2$) and comparable to that observed in a metallic manganite $\text{Nd}_{0.45}\text{Sr}_{0.55}\text{MnO}_3$ in which a uniform ordering of $d_{x^2-y^2}$ is stabilized [1,15]. Thus, an orbital/band polarization may well occur at the structural transition.

Recently, Anisimov *et al.* performed band calculations for $\text{Ca}_{2-x}\text{Sr}_x\text{RuO}_4$, using the LDA + U method [20]. Based on the difference in parity and in bandwidth between the d_{xy} and the $d_{yz,zx}$ orbital bands, they predict that the structural distortions first localize the latter orbitals and induce the above mentioned ferro-type ordering of $d_{yz} - d_{zx}$ orbitals at $x \sim 0.5$. While the bandwidth of the d_{xy} orbital band remains sufficiently large for metallic conduction, the localization and ordering of $d_{yz,zx}$ orbitals would stabilize local moments $S = 1/2$ and generate an AF coupling between them [20].

In order to further explore the electronic structure, we performed high magnetic field measurements for $x = 0.2$. Figure 3 shows the field dependence of M and the longitudinal magnetoresistance at 0.6 K. As B increases, M shows a stepwise increase at $B_{cr} = 2.3$ and 6 T for its ab -plane and c -axis components, respectively. These metamagnetic transitions should be due to the field

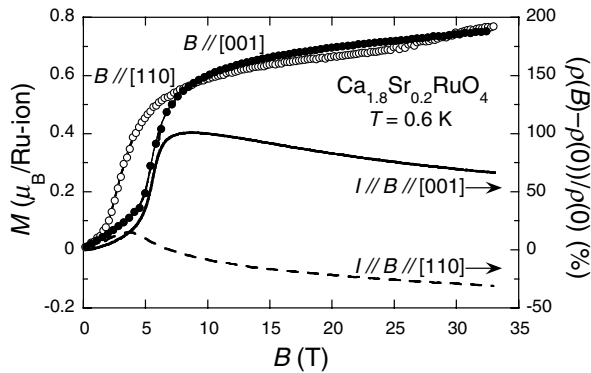


FIG. 3. Field dependence of the magnetization and longitudinal magnetoresistance at 0.6 K for $\text{Ca}_{1.8}\text{Sr}_{0.2}\text{RuO}_4$.

destabilization of the AF coupling. At the highest fields, both components show a tendency to saturate around $0.8\mu_B$ in sharp contrast with what is expected from band calculations. According to local density approximation, the band around the Fermi level is mainly composed of the $4d_{t_2g}$ orbitals [6,7]. For the Ru^{4+} state, the moment is expected to increase up to a saturation value of $2\mu_B$ until a half-metallic state is achieved, as reported for $\text{Sr}_{1-x}\text{Ca}_x\text{RuO}_3$ [29]. Nevertheless, the observed saturation moment is close to the effective magneton of $1\mu_B$ estimated from the Curie-Weiss analyses of $\chi(T)$ [14]. This suggests that the system at high fields is in an almost polarized FM state with a local moment of $S = 1/2$. In fact, both the ab -plane and c -axis components of the magnetoresistance change their signs from positive to negative across B_{cr} , which is consistent with a change in the spin coupling from AF to FM. Furthermore, the c -axis component increases by nearly 100% at B_{cr} in comparison with only 12% for the ab plane. This suggests that $d_{yz,zx}$ orbitals, which dominate the out-of-plane transport, are strongly involved in the metamagnetic transition, in comparison with d_{xy} orbitals, which are expected to govern the in-plane transport. All these results for $x = 0.2$ agree with the partial Mott gap scenario that predicts $S = 1/2$ localized moments in $d_{yz,zx}$ orbitals [20]. Thus, the decrease in γ_e for $x < 0.5$ suggests that the gap starts to open around $x = 0.5$. The strong narrowing of the itinerant d_{xy} band due to the tilt distortion as well as the scattering of carriers by these local moments may be the origin of the large enhancement of A near the Mott transition.

In conclusion, measurements in $\text{Ca}_{2-x}\text{Sr}_x\text{RuO}_4$ reveal the evolution from the spin-triplet superconductor Sr_2RuO_4 to a FM instability leading to a heavy-mass Fermi liquid state and eventually to a FM cluster glass. This itinerant FM coupling should be of Stoner-type, most likely due to the van Hove singularity of the d_{xy} band [6,7,14,16]. As the system further approaches the Mott transition, the AF correlation of localized moments with $S = 1/2$ develops, suppressing the magnetization and specific heat, while inducing a divergence of the in-plane scattering rate. We argue that the strong band narrowing due to the tilt distortion suppresses the d_{xy} band

Stoner-like FM. This stabilizes the AF correlated metal with a partial correlation gap in $d_{yz,zx}$ bands before a full gap opens at the Mott transition. These results underline the orbital dependent physics inherent to single layered ruthenates and point to the possible influence of the FM instability in the spin-triplet pairing.

The authors acknowledge T. Ishiguro, K. Ishida, M. Sigris, K. Yamada, H. Fukazawa, and S. McCall for comments. This work is supported by a Grant-in-Aid for Scientific Research from the Ministry of Education, Science, Sports and Culture of Japan, by NSF through the NSF Cooperative Agreement No. DMR-9527035, and by the State of Florida. S. N. has been supported by JSPS.

- [1] Y. Tokura and N. Nagaosa, *Science* **288**, 462 (2000).
- [2] Y. Maeno *et al.*, *Nature (London)* **372**, 532 (1994).
- [3] For a review, see Y. Maeno, T. M. Rice, and M. Sigris, *Phys. Today* **54**, No. 1, 42 (2001).
- [4] Y. Maeno *et al.*, *J. Phys. Soc. Jpn.* **66**, 1405 (1997).
- [5] A. P. Mackenzie *et al.*, *Phys. Rev. Lett.* **76**, 3786 (1996).
- [6] I. I. Mazin and D. J. Singh, *Phys. Rev. Lett.* **82**, 4324 (1999); *Phys. Rev. Lett.* **79**, 733 (1997).
- [7] Z. Fang and K. Terakura, *Phys. Rev. B* **64**, 020509(R) (2001).
- [8] Y. Sidis *et al.*, *Phys. Rev. Lett.* **83**, 3320 (1999).
- [9] T. Kuwabara and M. Ogata, *Phys. Rev. Lett.* **85**, 4586 (2000); M. Sato and M. Kohmoto, *J. Phys. Soc. Jpn.* **69**, 3505 (2000).
- [10] T. Imai *et al.*, *Phys. Rev. Lett.* **81**, 3006 (1998).
- [11] H. Mukuda *et al.*, *J. Phys. Soc. Jpn.* **67**, 3945 (1998).
- [12] D. F. Agterberg, T. M. Rice, and M. Sigris, *Phys. Rev. Lett.* **78**, 3374 (1997); M. E. Zhitomirsky and T. M. Rice, *Phys. Rev. Lett.* **87**, 057001 (2001).
- [13] T. M. Rice and M. Sigris, *J. Phys. Condens. Matter* **7**, L643 (1993); K. Miyake and O. Narikiyo, *Phys. Rev. Lett.* **83**, 1423 (1999); T. Nomura and K. Yamada, *J. Phys. Soc. Jpn.* **71**, 1993 (2002).
- [14] S. Nakatsuji and Y. Maeno, *Phys. Rev. Lett.* **84**, 2666 (2000); *Phys. Rev. B* **62**, 6458 (2000); *J. Solid State Chem.* **156**, 26 (2001).
- [15] O. Friedt *et al.*, *Phys. Rev. B* **63**, 174432 (2001).
- [16] A. Gukasov *et al.*, *Phys. Rev. Lett.* **89**, 087202 (2002).
- [17] S. Nakatsuji *et al.*, *J. Phys. Soc. Jpn.* **66**, 1868 (1997).
- [18] C. S. Alexander *et al.*, *Phys. Rev. B* **60**, R8422 (1999).
- [19] T. Mizokawa *et al.*, *Phys. Rev. Lett.* **87**, 077202 (2001).
- [20] V. I. Anisimov *et al.*, *Eur. Phys. J. B* **25**, 191 (2001).
- [21] T. Hotta and E. Dagotto, *Phys. Rev. Lett.* **88**, 017201 (2002).
- [22] F. Nakamura *et al.*, *Phys. Rev. B* **65**, 220402(R) (2002).
- [23] K. Kadowaki and S. B. Woods, *Solid State Commun.* **58**, 507 (1986).
- [24] S. Kondo *et al.*, *Phys. Rev. Lett.* **78**, 3729 (1997).
- [25] R. Jin *et al.*, *cond-mat/0112405*.
- [26] S. R. Julian *et al.*, *Physica (Amsterdam)* **259-261B**, 928 (1999).
- [27] J. R. Schrieffer, *J. Appl. Phys.* **39**, 642 (1968).
- [28] K. Ishida *et al.* (unpublished).
- [29] T. Kiyama *et al.*, *J. Phys. Soc. Jpn.* **68**, 3372 (1999).